

Specific heat and magnetization of the superconducting monoxides: NbO and TiO[†]

Ali M. Okaz* and P. H. Keesom

Physics Department, Purdue University, West Lafayette, Indiana 47907

(Received 27 May 1975)

The specific heat of five NbO_x samples (x between 0.96 and 1.02) is reported for the Meissner, mixed, and normal states. The specific heat of seven TiO_x samples, covering the range of composition from 0.91 to 1.17, is discussed and compared to previous work. For NbO, the transition temperature T_0 reaches a maximum of 1.61 K near $x = 1.0$; for TiO, the transition temperature is not a function of composition. The densities of states of both systems are derived from the coefficients of the electronic specific heat γ and compared to the band-structure calculations. While NbO is found to be a low- κ intrinsic type-II superconductor, TiO is a high- κ dirty type-II material. Magnetization measurements on six NbO_x samples indicate that a deviation of stoichiometry by 1 at.% on the low oxygen side produces a multiphase system; the majority of such a sample is NbO and the minor phase is free Nb metal with a transition temperature around 6 K. Although magnetization data indicate too large a fraction for the minor phase, specific-heat data show a more reasonable value for this fraction.

I. INTRODUCTION

During the past twenty years, there have been extensive investigations on the superconductivity of the B1 structure carbides and nitrides of transition elements such as NbC, NbN, VN, and TiN.¹⁻³ Less attention, however, has been given to the transition-metal monoxides of niobium, vanadium, and titanium which belong to the same crystal structure. Previous investigations⁴⁻¹¹ showed that TiO and NbO possess metalliclike properties and become superconductive around 1 K. The third monoxide VO, although also metallic at room temperature, does not appear to become superconductive down to the millidegrees region.^{8,12}

Most of the electrical and some of the superconducting properties of both TiO and NbO have been previously investigated,⁴⁻¹⁰ but there are sizable discrepancies between different reported results, especially in terms of electrical resistivity and transition temperature in both magnitude and behavior as a function of composition. In TiO_x, there exists an extraordinarily wide range of composition ($0.8 \leq x \leq 1.3$) for which its structure is stable. The system is stabilized by an equilibrium concentration of vacancies (about 15%) which are randomly distributed on both titanium and oxygen sublattices. It is generally believed that the random distribution of vacancies is the cause for the conflict between different results. Goodenough¹³ has studied the influence of atomic vacancies on the properties of the transition-metal oxides, TiO and VO. He argued that isolated cation vacancies tend to trap two holes, and anion vacancies tend to trap two electrons. Although there is no direct evidence of the trapping mechanism, Goodenough used this trapping model to explain the peculiar properties of these monoxides.

In a review article by Banus *et al.*,¹² the electric, magnetic, and superconducting properties of TiO and VO were summarized and discussed.

NbO is different from TiO in having 25% ordered vacancies on both niobium and oxygen sublattices, and it exists only over a very narrow homogeneity range.¹⁴ Based on lattice-parameter measurements, Pollard⁶ has put the limits for single-phase NbO_x to be $0.98 \leq x \leq 1.02$. Hulm *et al.*⁸ reported that composition deviation by as little as 0.5 at.% on either side of stoichiometric NbO produces a mixed-phase sample. The present investigation tends to confirm this latter result.

No specific-heat study has been reported for TiO or NbO either in the normal or in the superconducting state. It was felt that specific-heat measurements in these two states would give information on some important parameters such as the density of states at the Fermi energy, the Debye temperature, and the transition temperature. Also, specific-heat measurements in constant magnetic fields would yield a thermodynamic description of the mixed state.

This study includes data on specific heat in the Meissner, mixed, and normal states for five different NbO_x samples (x between 0.96 and 1.02) and a comparison with different theories is made. Magnetization results of six samples are presented and compared with specific heat. The phase diagram of NbO is discussed in terms of the present results and compared to that given by Elliott¹⁴ and by Hulm *et al.*⁸ The resistivity measurements indicate that the samples used in the present work are more pure than those used by Pollard⁶ and Hulm *et al.*, while the transition temperatures are higher by about 0.2 K than previously reported.^{6-8,10} The dependence of T_0 on x agrees qualitatively with that given by Pollard, which is in contra-

diction with the work of Hulm *et al.* NbO is found to have a Ginzburg-Landau parameter κ of about 1.5 and is an intrinsic type-II superconductor.

The normal-state properties of seven TiO_x samples of different compositions (x between 0.91 and 1.17) are given and compared with previous theoretical and experimental work. From the electronic contribution to the specific heat, the density of states at the Fermi surface is calculated for different compositions and compared with band-structure calculations.^{15,16} An estimate of the Ginzburg-Landau parameter κ was obtained from the mixed-state results and is in good agreement with the Gor'kov-Goodman predictions for dirty type-II superconductors. The present results give much higher values of κ as compared to that found from magnetic susceptibility data reported by Hulm *et al.*⁸

II. EXPERIMENTAL

A. Specific heat and thermometry

Specific-heat measurements were done using a conventional ³He refrigerator for temperatures above 0.4 K and a dilution refrigerator for the very low temperature part. For specific heat, a standard heat pulse technique was employed. Two commercial germanium thermometers were used for temperature measurements below 4.2 K. One had been calibrated previously¹⁷ between 0.45 and 1 K against ³He vapor pressure as a secondary thermometer (1962 ³He scale¹⁸), and down to 0.15 K using a cerium-magnesium-nitrate (CMN) thermometer whose susceptibility was measured with a superconducting quantum interference device (SQUID). The temperature calibration of the other thermometer was based on the 1958 ⁴He scale¹⁹ for T between 1.2 and 4.2 K and on the 1962 ³He scale for T between 0.4 and 1.2 K. A third thermometer was in the form of an unencapsulated piece of germanium with four electrical leads of gold.²⁰ This thermometer has been calibrated between 2 and 10 K against a commercially calibrated germanium thermometer. Each thermometer was recalibrated in a magnetic field when it was used for the mixed-state measurements. Superconductive solenoids were used to produce the magnetic fields estimated to be accurate to about 2%.

In order to observe the effect of flux trapping and of sample magnetic history on the mixed-state properties, a set of measurements for each sample was performed using three different procedures A, B, and C. In procedure A, the field was applied after most of the cooling took place, to prevent flux trapping at H_{c1} . In procedures B and C, the field was applied before cooling, i.e., in the normal state. The measurement by procedure C was

done while allowing the sample to cool, but for B the sample was first cooled in the presence of the field and then measured upward in temperature.

The addenda included the thermometer, heater, glue, etc. The heat capacity of each of the commercial germanium thermometers was measured separately and the corrections due to the other constituents of the addenda were obtained using published data. The contribution of the addenda to the total heat capacity varied from 0.2 to 2% depending upon the sample and the temperature range. Above 2 K, this was approximately half of the lattice contribution of both NbO and TiO. An error in the lattice heat capacity should not exceed 5%. The systematic error was estimated to be less than 1% in the temperature range between 1 and 4 K and increased to about 2% at the lowest temperatures, owing mainly to temperature scale.

B. Samples

Six NbO and seven TiO samples were grown in the Central Materials Preparation Facility of Purdue University using the tri-arc technique. For NbO, niobium metal and niobium pentoxide (Nb₂O₅) powder in the proper stoichiometric amounts were mixed and melted in a crucible of high-density graphite. A detailed description of the crystal growing procedure has been given elsewhere.²¹ The NbO_x samples have the nominal compositions $x = 0.96, 0.98, 0.99, 1.00$ (No. 123), 1.00 (No. 120), and 1.02. One of the samples NbO_{1.00} (No. 123) was investigated after it has been annealed at about 1600 °C in gettered argon and then etched in CP₄ (HF: acetic acid: HNO₃: liquid bromine in the ratios 50:50:80:1). Dimensions of cylindrical NbO samples are typically 4–6 cm in height and have irregular diameters of about 3 mm.

For TiO, three of the samples (TiO_{0.95}, TiO_{1.00}, and TiO_{1.06}) have button shapes consisting of large crystal grains with some visible cracks on the surface. These three samples were annealed at about 1600 °C in gettered argon. The other four samples (TiO_{0.91}, TiO_{0.95}, TiO_{1.00}, and TiO_{1.17}) were grown by a pulling process and are approximately cylindrical in shape and of about 4 mm diam and 4 cm length.

An x-ray powder diffraction pattern was obtained for each of the three unannealed [NbO_{0.98}, NbO_{1.00} (No. 120), and NbO_{1.02}] samples using a diffractometer and Cu K α radiation. The patterns showed definitely a minor phase of Nb in the NbO_{0.98} sample and of NbO₂ in NbO_{1.02}. Very weak lines were poorly identified as belonging to Nb and NbO₂ in NbO_{1.00} (No. 120), but it is doubtful that this sample has more than one phase. X-ray data²² for the annealed NbO_{1.00} sample are given in Table I, and were obtained from a powder diffraction spectrum

using a Debye-Scherrer camera and Cu $K\alpha$ radiation. Mass-spectrographic analysis²² was made on this annealed sample with the results of the following principal impurities [in parts per million by weight (ppmw)]: Fe-10, Ta-50, W-20; all others are much less than 5 ppmw.

The analysis on TiO showed that all samples deviate from cubic structure as indicated by extra, fuzzy, unidentified lines in the x-ray patterns. This is an indication of a multiphase system. The button-shaped sample $TiO_{1.06}$ was analyzed with a mass spectrograph,²² which gave the following principal impurities (in ppmw): Al-30, Si-50, V-30, Fe-20, W-30; all others are much less than 10 ppmw. Semiquantitative analysis²² on the rod-shaped sample $TiO_{1.00}$ is also given in Table I. The lattice parameter a_0 was calculated for all the samples using the x-ray lines which represent the cubic phase. Some of the values of a_0 are in good agreement with those reported by other investigators,^{8, 11, 12, 23}

C. Electrical resistivity

The electrical resistivities of five NbO_x and four TiO_x samples were measured by a standard four-probe technique with measuring currents of 1 and 2 A. Table II summarizes the results of all samples measured at three fixed temperatures: 300, 77, and 4.2 K. As has already been established, both NbO and TiO have metalliclike properties.

The present results agree with previous investigations in terms of the behavior of the resistivity as a function of temperature. For NbO, the resistivity decreases with decreasing temperature, while for TiO it increases with decreasing temperature except for the stoichiometric composition where the resistivity is nearly constant. The high resistivity of TiO as compared to metals and also to NbO can probably be explained by the large concentration of randomly distributed lattice vacancies. The residual resistivities of three NbO_x samples (the first three samples in Table II) are several orders of magnitude lower than those of the other two NbO_x samples ($x \geq 1.0$)

TABLE I. X-ray analysis of the annealed $NbO_{1.00}$ and the rod $TiO_{1.00}$ samples.

Sample	Phase	Structure	Estimated presence line strength (%)	
Annealed	NbO	sc	Very strong	> 90
$NbO_{1.00}$ (No. 123)	Nb	bcc	Weak	< 10
	Unknown		Very very weak	< 5
$TiO_{1.00}$ (No. 172B)	TiO	fcc	Very strong	> 90
	TiO	Monoclinic	Very weak	< 10
	Ti	Hexagonal	Very weak	< 5

TABLE II. Electrical resistivity of five NbO_x and four TiO_x samples.

Sample	Sample number	Resistivity ($\mu\Omega$ cm)			$\Gamma = \frac{R_{300}}{R_{4.2}}$
		300 K	77 K	4.2 K	
$NbO_{0.98}$	126	18.05	1.96	0.36	50.1
$NbO_{1.00}$	123	19.11	2.24	0.14	136.5
$NbO_{1.00}$ ^a	123	17.71	1.51	0.10	171.1
$NbO_{1.00}$	120	21.13	3.56	1.74	12.1
$NbO_{1.02}$	127	19.78	4.00	2.27	8.7
$TiO_{0.91}$	172A	311.9	336.3	344.9	0.90
$TiO_{0.95}$	182B	289.4	289.4	292.2	0.99
$TiO_{1.00}$	172B	283.9	259.4	256.2	1.11
$TiO_{1.17}$	182A	425.3	452.9	483.2	0.67

^aAnnealed.

which are about identical to published data.^{6, 8, 24}

D. Magnetization

Magnetization measurements were done in a pumped 4He bath at constant temperature. The sample was moved rapidly from one 5000-turn coil to a second identically, but oppositely, wound coil 6 cm away. This induces a deflection of a ballistic galvanometer which is directly proportional to the magnetization. The accuracy of the measurement was limited by the sensitivity of the galvanometer and the stability of the magnetic field. The perfect diamagnetic part of the Meissner state was used for calibration in these measurements.

III. RESULTS AND DISCUSSION

A. Specific heat of NbO

The normal-state results of the annealed $NbO_{1.00}$ sample are plotted as C/T vs T^2 in Fig. 1. The

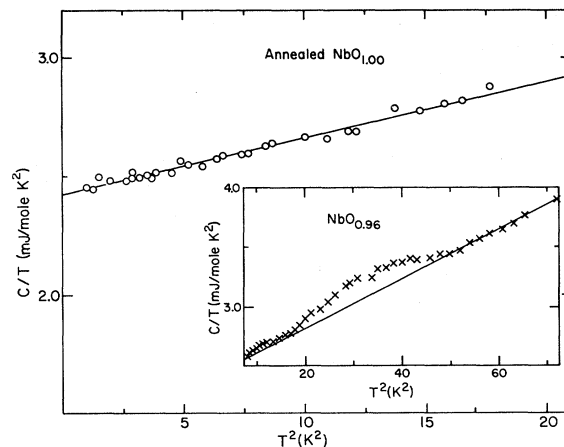


FIG. 1. Specific heat of annealed $NbO_{1.00}$ in the normal state plotted as C/T vs T^2 . Inset is the specific heat of $NbO_{0.96}$ between 3 and 9 K in which the solid line was obtained from measurements below 4.2 K.

normal-state data were taken in zero field as well as in a field of 300 Oe, which was sufficient to drive the sample normal down to the lowest temperature. The inset in Fig. 1 represents the data for the $\text{NbO}_{0.96}$ sample in zero field between 3 and 9 K. The normal state specific heat can be expressed in the form

$$C_n = \gamma T + \alpha T^3, \quad (1)$$

where γ and α are the coefficients of the electronic and lattice contributions, respectively.

The values of γ and of the Debye temperature Θ_0 at 0 K for this annealed sample and for other investigated samples are listed in Table III. Each value of γ was obtained by extrapolating the specific heat in a plot of C/T vs T^2 down to 0 K and was adjusted within the experimental error such that the entropies of the normal and Meissner states were equal at the transition temperature T_0 .

As can be seen from Table III, the coefficient of the electronic specific heat γ increases by about 2% when x increases by the same percentage. However, the accuracy of the measurements is of the order of 1%, so that the linear relation between γ and x is not conclusive. Also, the presence of superconducting Nb in composition for one side of stoichiometry and insulating NbO_2 for the other side makes it difficult to correlate γ with x . Nevertheless, the increase of the oxygen content could lead to a small increase in the electron concentration in the conduction band and probably corresponds to a small increase in γ .

The lattice specific heat is very small as compared to the electronic contribution, which makes it difficult to determine accurate values for α and consequently for Θ_0 . The best estimate of Θ_0 for all NbO_x compositions is 550 K, with an error of $\pm 5\%$. This value of Θ_0 is higher by 20% than that calculated by Kaufmann²⁵ using Lindeman's relation at high temperatures, which has a possible error of $\pm 10\%$.

The coefficients of the electronic specific heat γ gives a direct measure of the density of states at the Fermi surface $N_\nu(0)$. The quantity $N_\nu(0)$ is the enhanced density of states by the electron phonon interactions, a well-known feature of the transition metals and their alloys. The experimental coefficient γ is related to the so-called "bare" coefficient γ_{bs} by the expression²⁶

$$\gamma = \frac{2}{3} \pi^2 k_B^2 N_\nu(0) = \gamma_{bs} m^*/m^* \quad (2)$$

where

$$\gamma_{bs} = \frac{2}{3} \pi^2 k_B^2 N_{bs}(0) \quad (3)$$

and

$$m^*/m^* \approx 1 + N_{bs}(0) V_{ph}. \quad (4)$$

TABLE III. Normal-state specific-heat results of five NbO_x samples.

Sample	γ (mJ/mole K ²)	α (μ J/mole K ⁴)	Θ_0 (K)
$\text{NbO}_{0.96}$	2.38	21	570
$\text{NbO}_{0.98}$	2.36	28	520
$\text{NbO}_{1.00}$	2.42	8	780 ^a
$\text{NbO}_{1.00}^b$	2.43	24	550
$\text{NbO}_{1.02}$	2.46	10	730 ^a

^aThese high values of Θ_0 are due mainly to the uncertainty in the addenda correction.

^bAnnealed.

In Eqs. (3) and (4), $N_{bs}(0)$ is the density of states that would be given by an exact band-structure calculation, and is different from the free-electron density of states only through the static electron-ion interactions. V_{ph} is the matrix element of the electron-electron interaction, mediated by phonons, which enhance $N_{bs}(0)$ by a factor m^*/m^* or equivalently by the factor $(1 + \lambda)$, where λ is the coupling constant introduced by McMillan.²⁷

The coupling constant λ can be expressed in terms of the measurable parameters T_0 and Θ_0 and the Coulomb pseudopotential strength μ^* as²⁷

$$\lambda = \frac{1.04 - \mu^* \ln(\Theta_0/1.45T_0)}{(1 - 0.62\mu^*) \ln(\Theta_0/1.45T_0) - 1.04}. \quad (5)$$

The value of λ for each composition has been calculated using T_0 and Θ_0 and assuming μ^* to be equal to 0.1.³ The average value of λ is 0.37, which gives for $N_{bs}(0)$ the average value 0.37 states/(eV atom) for single spin direction and yields a value for V_{ph} of about 1.0 eV. Recent band-structure calculations by Wahnsiedler²⁸ give for $N_{bs}(0)$ the value 0.27 states/(eV atom), which is in reasonable agreement with the experimental value given above. Although the density of states at the Fermi surface of NbO is about equal to that of NbN,³ V_{ph} of the latter is from three to four times higher, and this, then, is the main reason that NbO has a much lower transition temperature than NbN.

The superconducting state results in zero field for the $\text{NbO}_{0.96}$ sample are displayed in Fig. 2. The specific heat has the form

$$C_s = C_{ls} + C_{es}, \quad (6)$$

where C_{ls} is the lattice contribution and is assumed to be identical to C_{ln} ($= \alpha T^3$). The electronic contribution C_{es} may be approximated according to the BCS theory, for $T < 1/2 T_0$, by

$$C_{es} = a\gamma T_0 e^{-bT_0/T}, \quad (7)$$

where a and b are constants. By plotting $\ln(C_{es}/\gamma T_0)$ vs T_0/T , the constants a and b for each

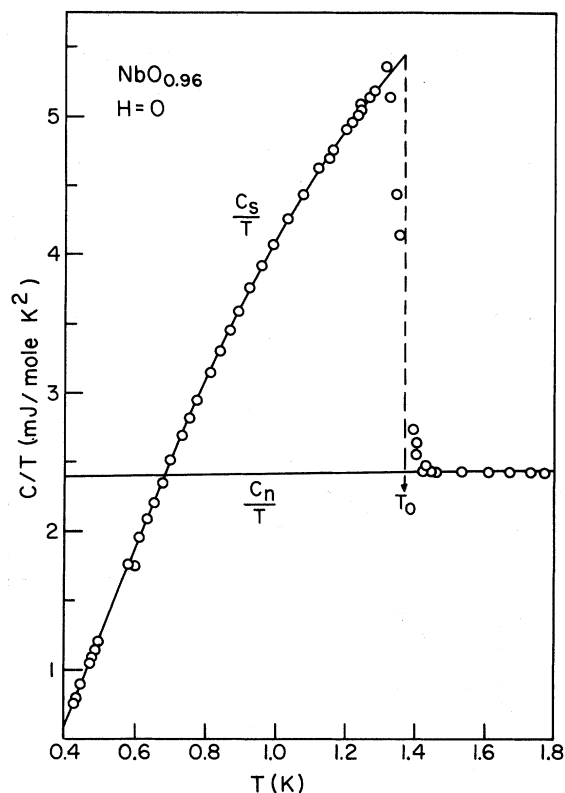


FIG. 2. Specific heat of $\text{NbO}_{0.96}$ in the superconducting (C_s) and normal (C_n) states, plotted as C/T vs T .

sample are determined; they are listed in Table IV. The transition temperature T_0 , the transition width ΔT_0 , and the specific-heat ratio $C_{es}/\gamma T_0$ at T_0 for the different compositions are also listed in Table IV. The BCS values are included for comparison. As can be seen, the Meissner state parameters are in poor agreement with those following from the BCS theory, but are comparable to those found for most compounds and alloys.

The dependence of the transition temperature T_0 on the oxygen-to-niobium ratio is qualitatively similar to that found by Pollard.⁶ The transition temperature reaches a maximum near stoichiome-

try and decreases on both sides. Quantitatively, the value of T_0 for $x \leq 1.0$ is higher than that measured by Pollard, but is nearly identical for $x = 1.02$. Hulm *et al.*⁸ reported a constant value ($T_0 = 1.38$ K) for stoichiometric and oxygen-rich compositions, but when there is a deviation by as little as 0.5 at. % on the low-oxygen side, T_0 rises sharply to 6 K and then levels off at 7 K near $x = 0.5$. They attributed this increase in T_0 to the presence of free niobium metal and pointed out, in addition, that (1–2)-at. % oxygen is dissolved in the niobium phase and thus depresses the transition temperature of niobium below 9.2 K, according to the work of DeSorbo.²⁹ The present results are not in agreement with those of Hulm *et al.*, as both $\text{NbO}_{0.98}$ and $\text{NbO}_{0.96}$ samples show superconducting properties near 1.5 K which are completely similar to those of the stoichiometric samples; only a very small fraction of the sample becomes superconductive at about 6 K. Most probably, though, Hulm *et al.* did not extend their measurements down to very low temperatures to observe the main transition near 1.5 K.

Making use of the well-known thermodynamic formulas, the critical-field curve $H_c(T)$ was derived from the specific-heat data. Table IV gives for each composition the calculated $H_c(0)$ and the initial slope of the critical field derived from the Rutgers formula

$$\frac{\Delta C}{T} \Big|_{T_0} = \frac{V_m}{4\pi} \left(\frac{dH_c(T)}{dT} \Big|_{T_0} \right)^2, \quad (8)$$

where ΔC is the specific-heat jump in zero field ($C_s - C_n$) at the transition and V_m is the molar volume which was calculated from a room-temperature density⁶ of 7.24 g/cm³ but increased to 7.25 g/cm³ to take care of thermal contraction. Table IV gives also the superconducting energy gap at 0 K estimated from the BCS relation

$$\frac{2\Delta_d(0)}{k_B T_0} = \frac{4\pi}{\sqrt{3}} \left(\frac{H_c^2(0) V_m}{8\pi \gamma T_0^2} \right)^{1/2}, \quad (9)$$

where d refers to d -electrons.

TABLE IV. Meissner-state specific-heat parameters of five NbO_x samples.

Sample	T_0 (K)	ΔT_0 (mK)	$\frac{C_{es}(T_0)}{\gamma T_0}$	a	b	$\frac{2\Delta(0)}{k_B T_0}$	$H_c(0)$ (G)	$-\left(\frac{dH_c}{dT}\right)_{T_0}$ (G/K)
$\text{NbO}_{0.96}$	1.37	50	2.25	7.2	1.33	3.43	129.7	158.2
$\text{NbO}_{0.98}$	1.55	60	2.19	4.5	1.10	3.32	141.1	154.3
$\text{NbO}_{1.00}$	1.55	58	2.13	5.0	1.14	3.34	143.6	151.5
$\text{NbO}_{1.00}^a$	1.61	50	2.15	4.2	1.07	3.30	147.6	153.3
$\text{NbO}_{1.02}$	1.38	50	2.20	6.6	1.27	3.42	131.0	156.8
BCS theory			2.43	8.5	1.44	3.52		

^aAnnealed.

The results of the mixed-state specific heat are divided into two groups according to whether the external applied field H is larger or smaller than $H_{c1}(0)$. For $H < H_{c1}(0)$, the results are displayed in Fig. 3 as C/T vs T for the $\text{NbO}_{1.02}$ sample. The specific heat coincides with the zero-field curve until at a certain temperature T_1 , depending on the applied field, it smoothly departs upward. Just above this temperature there is a very sharp peak at T'_1 followed by a rapid decrease of the mixed-state specific heat. There are two choices for H_{c1} , either $H_{c1}(T_1)$ or $H_{c1}(T'_1)$, both of which are operational; however, the second choice is more uncertain than the first owing to hysteresis and internal heating effects which delay the appearance of the peak. The specific heat C_m drops sharply just after T'_1 , and therefore decreases slower over an interval ΔT_2 until it reaches C_n . The transition temperature T_2 is taken as the middle of this temperature interval ΔT_2 and is used to determine the upper critical field as $H_{c2}(T_2) = H$, the applied field. The uncertainty in estimating T_2 is about ΔT_2 .

In looking at Fig. 3, one could conclude that NbO is a type-I superconductor, as it shows one specific-heat peak which corresponds to a first-order transition, but smeared out over a finite temperature range. However, the temperature of the peak, T'_1 , is well above the temperature deduced

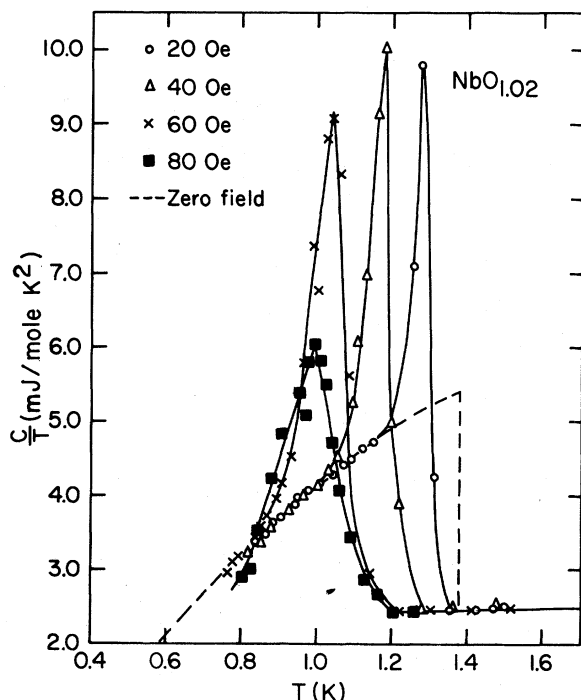


FIG. 3. Specific heat of $\text{NbO}_{1.02}$ for $H < H_{c1}(0)$, plotted as C/T vs T . Dashed curve represents the specific heat in zero field.

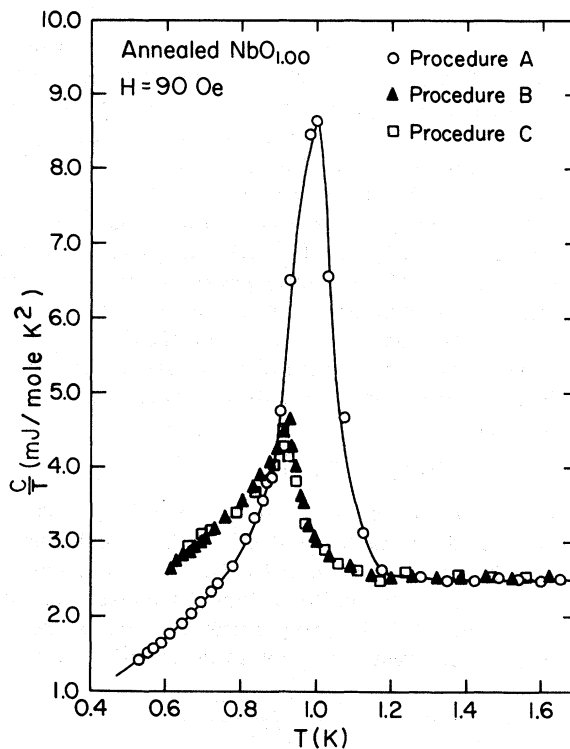


FIG. 4. Specific heat of annealed $\text{NbO}_{1.00}$ in a field of 90 Oe for three different procedures (see text), plotted as C/T vs T .

from the thermodynamic critical field $H_c(T)$. Second, as will be shown later, the specific-heat results for fields larger than $H_c(0)$, as well as the magnetization measurements on these samples, definitely indicate type-II behavior.

The mixed-state specific heat shows irreversibility near the temperature T'_1 , as the position and magnitude of the peak were not reproduced when the field was on during the cooling (procedures B and C), as is shown in Fig. 4 for $H = 90$ Oe in the case of the annealed $\text{NbO}_{1.00}$ sample. The effect is due to incomplete flux expulsion during the cooling in the presence of a field. The trapped flux is indicated by the increase of the specific heat above the zero-field value for $T < T_1$ and by the small shift of the peak towards lower temperatures. Also, the peak is smaller than that of procedure A. Furthermore, near the transition to the normal state, the specific-heat results of procedure A do not coincide with those of procedures B and C. From the above, it is clear that the mixed state is history dependent not only around H_{c1} , but also near H_{c2} , in contrast with pure Nb and V measurements.^{30,31} For $T > 1.0$ K and $H \leq 80$ Oe, the specific-heat jump cannot be resolved from the peak. Since the mixed-state range of temperature is very narrow for low magnetic fields, it is possible that a detailed measurement of the jump can-

not be performed.

For magnetic fields larger than $H_{c1}(0)$, only one critical temperature, T_2 , can be observed, since the mixed state persists down to 0 K. The results of this group of measurements for the $\text{NbO}_{1.02}$ sample are shown in Fig. 5, in which C/T vs T^2 is plotted. The upper critical-field $H_{c2}(T)$ curve is shown in Fig. 6 along with $H_c(T)$ and $H_{c1}(T)$ curves for $\text{NbO}_{1.02}$. The indicated experimental error in $H_{c2}(T)$ is mainly governed by the uncertainty in determining T_2 which results from irreversibilities near the upper critical field.

The upper critical field H_{c2} is usually expressed in terms of the dimensionless parameter $\kappa_1(t)$ by the equation³²

$$\sqrt{2} H_c(t) \kappa_1(t) = H_{c2}(t) \quad (10)$$

where t is the reduced temperature T/T_0 . The ratio of the penetration depth λ_L to the coherence length ξ is a measure of the Ginzburg-Landau parameter κ , which for a type-II superconductor should be ≥ 0.707 . The parameter κ can be expressed in terms of measurable quantities as

$$\kappa = \lim_{t \rightarrow 1} \kappa_1(t) = \frac{1}{\sqrt{2}} \frac{(dH_{c2}/dT)_{T_0}}{(dH_c/dT)_{T_0}} \quad (11)$$

The value of κ for each composition is listed in Table V. The Ginzburg-Landau parameter of the pure material κ_0 is calculated using the experimen-

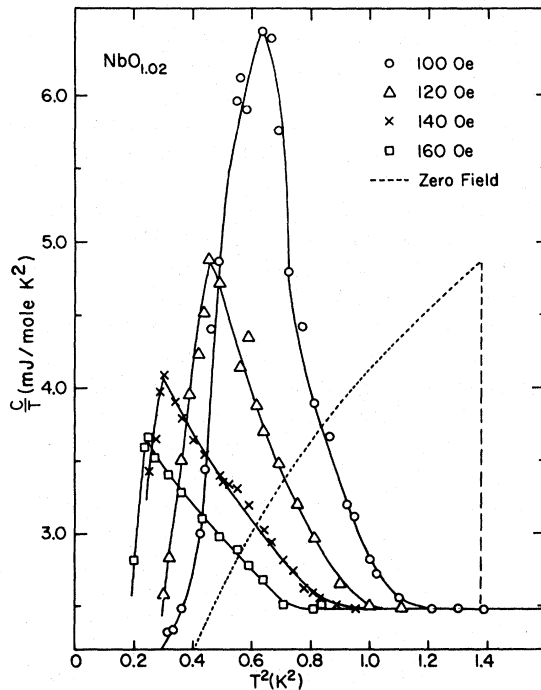


FIG. 5. Mixed-state specific heat of $\text{NbO}_{1.02}$ for $H > H_{c1}(0)$, plotted as C/T vs T^2 . Dotted curve represents the specific heat in zero field.

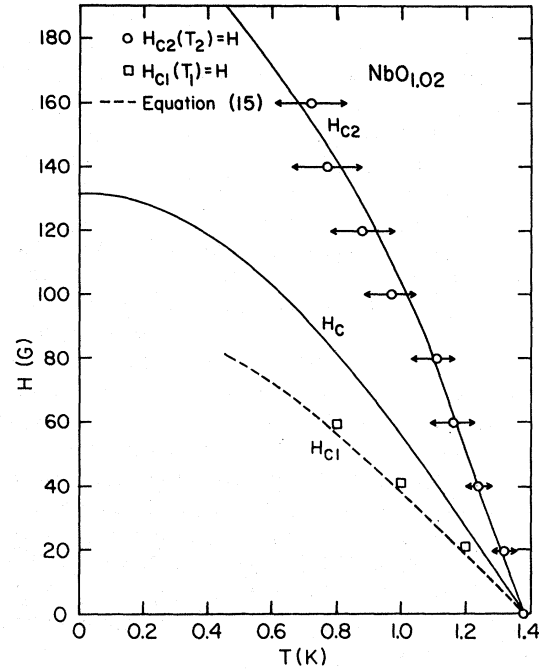


FIG. 6. Critical-field curves for $\text{NbO}_{1.02}$.

tal value of κ and the Gor'kov-Goodman relation³²

$$\kappa = \kappa_0 + \kappa_1 \quad (12)$$

where κ_1 is a parameter which depends on the electron mean free path. In the case of most alloys and compounds, κ_1 is given by³²

$$\kappa_1 = 7.5 \times 10^3 \gamma^{1/2} \rho_0 \quad (13)$$

where ρ_0 is the residual resistivity of the impure material in ohm cm and γ is in units of $\text{erg/cm}^3 \text{K}^2$. The values of κ_0 and κ_1 are also listed for four NbO samples in Table V. The uncertainty in κ_0 is mainly governed by the uncertainties in ρ_0 and $(dH_{c2}/dT)_{T_0}$, and it is estimated to be on the order of $\pm 20\%$.

The results of the upper critical field are usually discussed by comparing the ratio $\kappa_1(t)/\kappa$ to various theoretical predications.³³⁻³⁵ However, Helfand and Werthamer³⁶ pointed out that such a comparison between theory and experiment con-

TABLE V. Values of the Ginzburg-Landau parameters for four NbO_x samples.

Sample	κ	κ_1	κ_0^a
$\text{NbO}_{0.98}$	1.55	0.10	1.54
$\text{NbO}_{1.00}$	1.49	0.04	1.45
$\text{NbO}_{1.00}^b$	1.50	0.03	1.47
$\text{NbO}_{1.02}$	1.29	0.69	0.60

^aPossible error in each value of κ_0 is about ± 0.15 .

^bAnnealed.

tains some uncertainty, depending on the choice of the thermodynamic critical field $H_c(T)$ in Eqs. (10) and (11). Some authors use $H_c(T)$ deduced experimentally, while others use the parabolic law for the temperature dependence:

$$h_c(t) = H_c(T) / H_c(0) = 1 - t^2.$$

A third method uses the critical-field curve calculated from the BCS theory by Mühlischlegel.³⁷ Helfand and Werthamer introduced still another method of comparison independent from the choice of $H_c(T)$. They defined a normalized parameter $h^*(t)$ as

$$h^*(t) = H_{c2}(t) / \left(\frac{-dH_{c2}(t)}{dt} \right)_{t=1}. \quad (14)$$

Figure 7 shows the experimental behavior of h^* as a function of the reduced temperature t for both $\text{NbO}_{1.02}$ and the annealed $\text{NbO}_{1.00}$ samples, together with the predictions of Helfand and Werthamer for the case of infinite mean free path. The result for $\text{NbO}_{1.02}$ is in fair agreement with the theoretical curve, while that for annealed $\text{NbO}_{1.00}$ is not. The discrepancy is mainly due to the irreversible behavior of the mixed state.

Figure 6 shows the experimental $H_{c1}(T)$ obtained, down to $t = 0.6$ K, from specific-heat results at

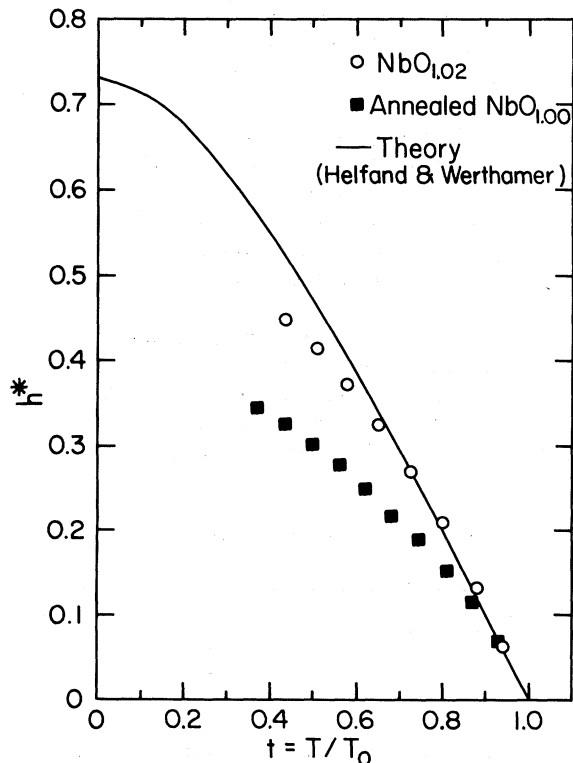


FIG. 7. Reduced upper critical field for $\text{NbO}_{1.02}$ and annealed $\text{NbO}_{1.00}$.

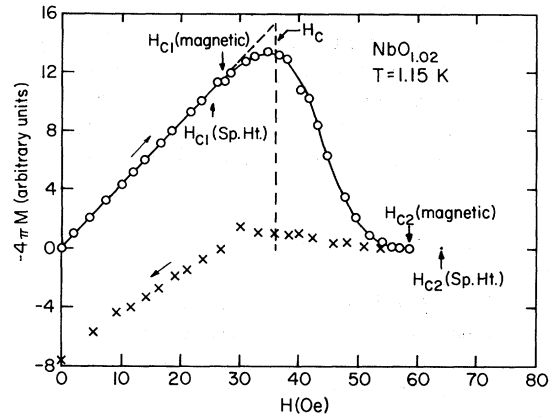


FIG. 8. Magnetization results of $\text{NbO}_{1.02}$ at 1.5 K for increasing and decreasing magnetic field.

constant applied field H . According to Harden and Arp,³⁸ H_{c1} can be expressed in the case of small- κ type-II superconductor ($1/\sqrt{2} < \kappa < 2$) by

$$H_{c1}(T) = 0.817 H_c(T) [\kappa_1(T)]^{-0.58}. \quad (15)$$

The values of $H_c(T)$ were deduced thermodynamically from zero-field specific-heat data. The experimental values of $\kappa_1(T)$ calculated from Eq. (10) are used. The values predicted by Eq. (15) are also displayed in Fig. 6; the agreement is very good.

As can be seen from Table V, the sample $\text{NbO}_{1.02}$ has $\kappa_0 = 0.60 \pm 0.15$, a value which is close to the critical limit for distinguishing between intrinsic or dirty type-II superconductors. The other three samples have κ_0 values well above the critical value 0.707, i.e., these samples show intrinsic type-II behavior. We conclude that the NbO system is a low- κ intrinsic type-II superconductor. The only known intrinsic type-II superconductors are the transition metals Nb and V, which can be obtained in very pure form, and certain intermetallic compounds such as the groups Nb_3X and V_3X .³⁹

B. Magnetization of NbO

Results of magnetization measurements in increasing as well as decreasing magnetic fields at constant temperature are shown in Fig. 8 for the $\text{NbO}_{1.02}$ sample. When the sample is in the Meissner state, i.e., $H < H_{c1}$ and $M = -(V/4\pi)H$, then the deflection D , which is proportional to M , is also proportional to H . Indeed, the initial part of the D -vs- H curve is linear, and this diamagnetic part is used to calibrate the measuring system. The values of H_{c1} and H_{c2} derived from the specific heat are marked on Fig. 8. The measurements on the unannealed stoichiometric sample $\text{NbO}_{1.00}$ (No. 120) gave magnetization results similar to the $\text{NbO}_{1.02}$ sample. In addition, the

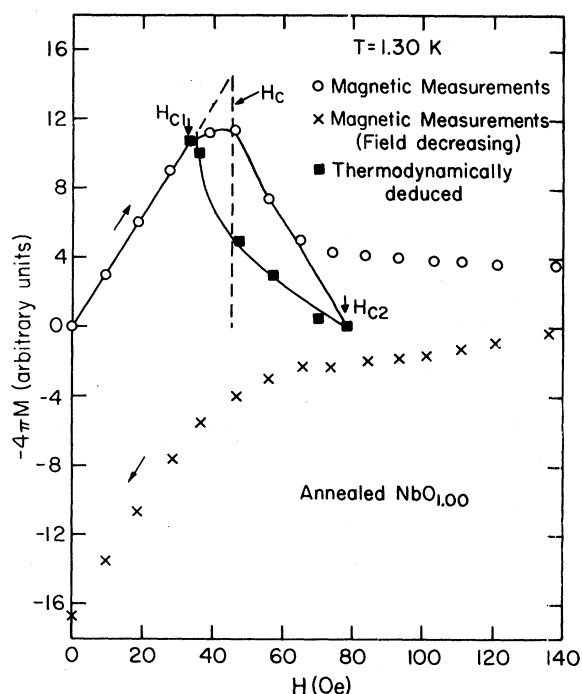


FIG. 9. Magnetization results of annealed $\text{NbO}_{1.00}$ at 1.30 K for increasing and decreasing magnetic field, together with the thermodynamically deduced magnetization.

results in a decreasing field indicate that the irreversibility in the mixed state is much less severe than for all other investigated samples. However, no specific-heat measurement was made on this sample.

Four other samples, the annealed $\text{NbO}_{1.00}$ and the unannealed $\text{NbO}_{0.98}$, $\text{NbO}_{0.98}$, and $\text{NbO}_{0.99}$ were also investigated. The results for the annealed $\text{NbO}_{1.00}$ at $T = 1.3$ K are given in Fig. 9. As can be seen, the magnetization does not go to zero at H_{c2} , but instead approaches a finite constant value as the applied field increases. In order to investigate the source of this additional magnetization, the measurements were repeated at 4.2 K, and at higher fields. After an initial diamagnetic part, the magnetization decreased very slowly and had not come to zero at 400 Oe. The magnetization results of the $\text{NbO}_{0.96}$, $\text{NbO}_{0.98}$, and $\text{NbO}_{0.99}$ samples shown similar behavior to

that observed for the annealed sample. The two samples $\text{NbO}_{0.99}$ and $\text{NbO}_{0.98}$ remained superconductive up to 600 and 850 Oe, respectively. Specific heat was measured for the $\text{NbO}_{0.98}$ in zero field as well as in a field of 8.3 kOe, up to 10 K. The zero-field results show that a very small fraction of the sample is superconductive, with very broad transition to the normal state, from 3 to 7 K (the inset of Fig. 1). Superconductivity is not destroyed by this high magnetic field, but shifts to slightly lower temperature.

Magnetization results indicate that while the unannealed $\text{NbO}_{1.00}$ (No. 120) and $\text{NbO}_{1.02}$ samples, show only one phase, all other samples have multiphase crystal structures. The sample $\text{NbO}_{1.02}$ behaves as a single phase in terms of the magnetic properties, since the insulating NbO_2 phase does not contribute to the magnetization. By comparing the perfect diamagnetic part of the annealed $\text{NbO}_{1.00}$ sample at 4.2 K to the data obtained at 1.3 K, it can be seen that approximately 10% of the sample still behaves magnetically as a superconductor at 4.2 K. This sample then has free niobium metal, probably in the form of filaments. The net weight-gain analysis on the annealed sample gave $x = 0.992$, which means that the sample has lost about 1% oxygen during the annealing process. Therefore it is expected that only 1% free niobium metal is formed. Magnetization results of $\text{NbO}_{0.96}$, $\text{NbO}_{0.98}$, and $\text{NbO}_{0.99}$ show similar behavior to that of the annealed $\text{NbO}_{1.00}$ sample; $\text{NbO}_{0.96}$ appears magnetically as if 40% of the sample is superconductive, while in the $\text{NbO}_{0.99}$ sample it is about 7%.

Magnetization can show too large a fraction of superconducting material if superconductive sheaths enclose normal regions, but this would not be the case for the specific heat, as this measures a bulk effect. The specific-heat results of annealed $\text{NbO}_{1.00}$ and $\text{NbO}_{0.96}$ between 2 and 10 K indicate that approximately 3% of each sample remains superconductive until about 7 K. This result is in qualitative agreement with the phase diagram given by Elliott¹⁴ and is consistent with x-ray data. Therefore NbO_x has a single phase only when $x = 1.0$, and more than one phase when x deviates from 1.0 by about 1 at. %.

TABLE VI. Results of normal-state specific heat of seven TiO_x samples.

x	Buttons			Rods			
	0.96	1.00	1.06	0.91	0.95	1.00	1.17
γ (mJ/mole K^2)	2.92	2.46	3.06	3.54	3.33	3.16	4.50
α ($\mu\text{J}/\text{mole K}^4$)	14.7	12.6	13.7	10.5	8.4	22.1	6.3
Θ_0 (K)	640	675	655	715	770	560	850

IV. SPECIFIC HEAT OF TiO

Specific-heat results in the normal state are summarized in Table VI for seven different TiO_x samples, where x ranges from 0.91–1.17. The entries in the table are the coefficients of the electronic contribution γ , and of the lattice contribution α , and the Debye temperature Θ_0 at 0 K derived from the values of α . As can be seen from Table VI, the lattice specific heat is very small as compared to the electronic contribution, which makes it difficult to get accurate values for the Debye temperature Θ_0 and to study its dependence on composition. The best value of Θ_0 for TiO is 650 K, which is in reasonable agreement with the Θ value reported by Kaufmann of 612 K, with possible error of $\pm 10\%$.²⁵

Down to 0.4 K no complete transition to the superconducting state was observed for four samples: the button-shaped $\text{TiO}_{0.95}$ and $\text{TiO}_{1.00}$ and the rod-shaped $\text{TiO}_{0.91}$ and $\text{TiO}_{1.17}$. Specific-heat results for these four samples are displayed as C/T vs T in Fig. 10. In order to get information about the superconducting state in zero field, the measurements have to be extended down to at least 0.1 K, since the transition width is estimated to be of the order of half a degree. As can be seen from Fig. 11, the stoichiometric rod $\text{TiO}_{1.00}$ sample showed a complete transition at approximately 0.5 K, but the measurement was not extended below 0.4 K. The transition occurs in two steps, indicating a double-phase crystal structure which is in agreement with x-ray data (see Table I).

The coupling constant λ has been estimated using Eq. (5) and the values of Θ_0 and T_0 deduced from specific-heat results of $\text{TiO}_{0.95}$ and $\text{TiO}_{1.06}$ (see Fig. 11). The average λ is about 0.37. Based on this value of λ and using Eqs. (2) and (4), the band-structure density of states $N_{bs}(0)$ have been calculated for the different composition. Figure 12 shows a graph of $N_{bs}(0)$ vs x in which

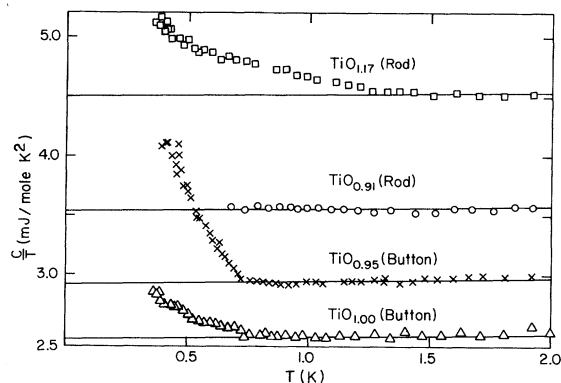


FIG. 10. Specific heat of four TiO_x samples in zero field, plotted as C/T vs T . Solid lines represent the specific heat in the normal state.

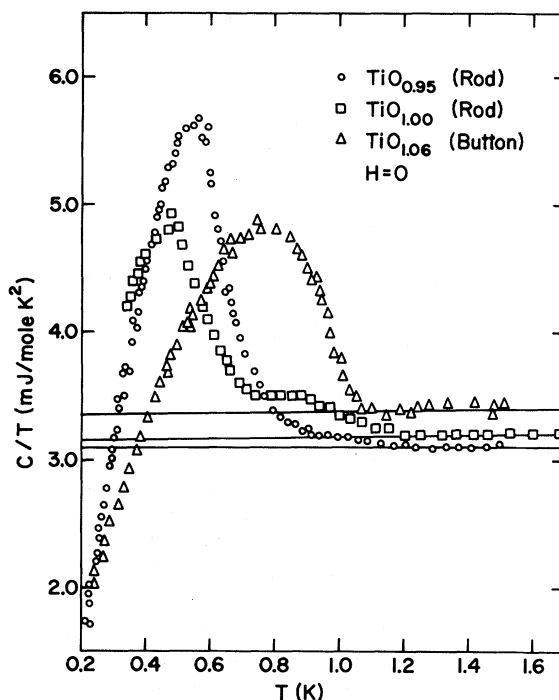


FIG. 11. Specific heat of three TiO_x samples in zero field, plotted as C/T vs T . Solid lines represent the specific heat in the normal state.

the results are divided into two groups: the button-shaped samples and the cylindrical-pulled samples. The experimental behavior of $N_{bs}(0)$, or equivalently γ , is about the same for the two groups, i. e., both show a minimum at $x=1.0$. The difference between the two sets of results can be understood, as the pulled samples are more dense and therefore contain less vacancies. This is in agreement with Shoen and Denker's theoretical calculations on the change in the density of states with vacancy concentration.¹⁶ As shown in Fig. 12, the experimental dependence of

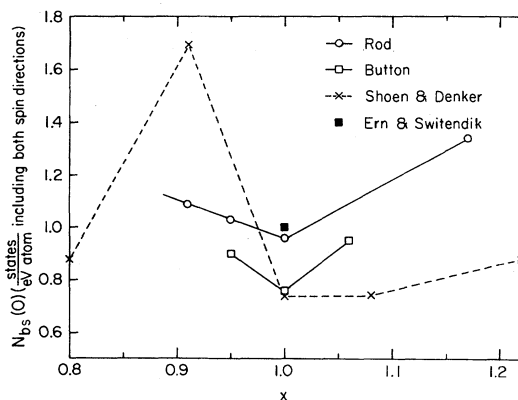


FIG. 12. Density of states at the Fermi surface for different compositions of TiO_x .

TABLE VII. Meissner- and mixed-state parameters for $\text{TiO}_{0.95}$ and $\text{TiO}_{1.06}$.

x	T_0 (K)	$\frac{C_{es}(T_0)}{\gamma T_0}$	a	b	$-\left(\frac{dH_{c2}}{dT}\right)_{T_0}$ (10^4 G/K)		κ	κ_1	$H_{c2}(0)$ (kG)
					This work	Ref. 8			
0.95	0.65	1.93	4.6	1.05	4.60 ± 0.20	0.37	210 ± 10	110	30, 5
1.06	0.94	1.61	2.0	0.66	3.47 ± 0.20	0.44	166 ± 10	105	32, 9

$N_{bs}(0)$ on x as compared to the theoretical one is substantially smaller for $x < 1.0$, and much larger for $x > 1.0$. The experimental behavior of γ as a function of x is also in qualitative agreement with the magnetic-susceptibility results reported by Denker.⁵ The susceptibility is larger for samples with x different from 1.00 than for stoichiometric compositions. Denker attributed this additional susceptibility to the decoupling of the spin system by odd or missing titanium atoms; the susceptibility increases because the titanium $3d$ orbitals have unpaired spins.

Hulm *et al.*⁸ reported much lower values of γ derived from their magnetic measurements on TiO. Also, their results showed that γ decreases with increasing x , which is in contradiction with the present results. The discrepancy is due to the difference in sample preparation, since Hulm *et al.* annealed their samples at 800 °C, which is below the transformation temperature of TiO; the crystal structure transforms into a monoclinic one by annealing below 1225 °C.^{11,40} In addition, they mentioned that the H_{c2} data from which γ was derived are somewhat uncertain.

The transition of $\text{TiO}_{1.06}$ from the normal to the Meissner state (see Fig. 11) is not sharp but gradual, and extends from 1.1 to 0.7 K, indicating multiphase crystal structures. For $\text{TiO}_{0.95}$, this transition is sharp as compared to the $\text{TiO}_{1.06}$ sample, excluding a long tail that has a small contribution to the total entropy. Although the specific-heat jump ($C_s - C_n$) at T_0 for $\text{TiO}_{0.95}$ is comparable to that of NbO, the transition is very wide and indicates a multiphase sample. The Meissner-state parameters of these two samples are listed in Table VII. The critical-field curve and its initial slope were deduced thermodynamically for each sample, and are found to differ from that calculated from the BCS theory. This is due to the very broad transition from the normal to the Meissner state which makes the calculations of $H_c(T)$ near T_0 , using entropy differences, less certain.

The wide transition observed for TiO is more or less similar to that reported by Hulm *et al.*⁸ and Reed *et al.*⁹ This investigation indicates that the transition temperature and its width are not determined by composition but much more by sample preparation. While the results of Hulm *et al.* showed a well-defined

maximum of T_0 (1.05 K) at $x = 1.07$, Reed *et al.* reported that T_0 is relatively independent of x and lies between 0.6 and 0.9 K for the whole range of composition. So it is not surprising that the present investigation gives results of the same magnitude as previously reported. Doyle *et al.*⁴¹ suggested that fluctuations of 1 and 2% in vacancy concentration are enough to change T_0 by (50–100)%. This implies that any comparison between different investigations is not very meaningful.

The mixed-state specific heat was measured in three different magnetic fields, much higher than $H_c(0)$, in order to get a reasonable shift of the transition from that in zero field. The samples were cooled in a constant field and then the measurements were performed upward in temperature. The transition from the mixed to the normal state is spread over a temperature interval ΔT_2 which increases as the magnetic field increases. The transition temperature T_2 was taken as the middle of the temperature interval ΔT_2 with an uncertainty not more than $\frac{1}{2}\Delta T_2$.

The upper critical-field curve near T_0 was derived from the mixed-state specific heat and was used to calculate the initial slope $(dH_{c2}/dT)_{T_0}$. The present work gives values for $(dH_{c2}/dT)_{T_0}$ which are about ten times higher than those found from magnetic-susceptibility measurements of Hulm *et al.*⁸ The values of κ derived from experiment $(dH_{c2}/dT)_{T_0}$ and using $(dH_c/dT)_{T_0}$ derived from the BCS theory are in reasonable agreement with the values of κ_1 calculated using the normal-state parameter γ and ρ_0 and Eq. (13). The upper critical field at 0 K, $H_{c2}(0)$, was also calculated using the value of κ and the expression following the Ginzburg-Landau-Abrikosov-Gor'kov theory for dirty type-II superconductors

$$H_{c2}(0) = 1.77 \kappa H_c(0) \quad , \quad (16)$$

in which $H_c(0)$ was obtained from the BCS theory. Table VII gives also the mixed-state parameters for the $\text{TiO}_{1.06}$ and $\text{TiO}_{0.95}$ samples. We conclude that the samples of TiO used in this investigation are high- κ dirty type-II superconductors.

V. SUMMARY

Niobium monoxide is a weak-coupling, low- κ intrinsic type-II superconductor. On the low-oxygen side a deviation by about 1 at. % from stoichi-

ometry produces multiphase crystal structures; the major phase is NbO with T_0 near 1.5 K, and the minor phase is free niobium metal with T_0 of about 6 K. Magnetization results for samples with $x < 1.0$ indicates a comparatively large fraction for the minor phase which arises from shielding effects, as specific heat results indicate a fraction in agreement with phase-diagram calculations.

Titanium monoxide is also a weak coupling superconductor, but with high- κ values due to the unusual high residual resistivity produced by the random distribution of lattice vacancies. The

transition temperature T_0 depends on the preparation of the sample, which produces composition gradients and consequently multiphase crystal structures. The coefficient of the electronic specific heat γ is determined as a function of composition; its behavior is in qualitative agreement with the theoretical calculations of Shoen and Denker.

ACKNOWLEDGMENTS

We thank Professor J. M. Honig for his continuous interest in this work and L. E. Wenger for his cooperation and valuable discussions.

[†]Work supported by the NSF (Grant No. DMR 7203090A2 and MRL Programs GH 33574A1 and DMR 7203018).

*Present address: Faculty of Engineering, Alexandria University, Alexandria, Egypt.

¹B. T. Matthias and J. K. Hulm, Phys. Rev. **87**, 799 (1952).

²G. F. Hardy and J. K. Hulm, Phys. Rev. **93**, 1004 (1954).

³T. H. Geballe, B. T. Matthias, J. P. Remeika, A. M. Clogston, V. B. Compton, J. P. Maita, and H. J. Williams, Physics (N.Y.) **2**, 293 (1966).

⁴A. D. Pearson, J. Phys. Chem. Solids **5**, 316 (1958).

⁵S. P. Denker, J. Appl. Phys. **37**, 142 (1966).

⁶E. R. Pollard, Ph.D. thesis (Massachusetts Institute of Technology, 1968) (unpublished).

⁷J. K. Hulm, C. K. Jones, R. Mazelsky, R. C. Miller, R. A. Hein, and J. W. Gibson, *Proceedings of the IXth International Conference on Low Temperature Physics*, edited by J. G. Daunt *et al.* (Plenum, New York, 1965), Part A, p. 600.

⁸J. K. Hulm, C. K. Jones, R. A. Hein, and J. W. Gibson, J. Low Temp. Phys. **7**, 291 (1972).

⁹T. B. Reed, M. D. Banus, M. Sjöstrand, and P. H. Keesom, J. Appl. Phys. **43**, 2478 (1972).

¹⁰H. R. Khan, C. J. Raub, W. E. Gardner, W. A. Fertig, D. C. Johnston, and M. B. Maple, Mater. Res. Bull. **9**, 1129 (1974).

¹¹M. D. Banus, Mater. Res. Bull. **3**, 723 (1968).

¹²M. D. Banus, T. B. Reed, and A. J. Strauss, Phys. Rev. B **5**, 2775 (1972).

¹³John B. Goodenough, Phys. Rev. B **5**, 2764 (1972).

¹⁴R. P. Elliott, Trans. Am. Soc. Met. **52**, 990 (1960).

¹⁵V. Ern and A. C. Switendick, Phys. Rev. **137**, A1927 (1965).

¹⁶J. M. Shoen and S. P. Denker, Phys. Rev. **184**, 864 (1969).

¹⁷Ali M. Okaz, Ph.D. thesis (Purdue University, 1975) (unpublished).

¹⁸T. R. Roberts, R. H. Sherman, and S. G. Sydorik, J. Res. Natl. Bur. Stand. (U.S.) A **68**, 567 (1964); R. H. Sherman, S. G. Sydorik, and T. R. Roberts, *ibid.* **68**, 579 (1964).

¹⁹F. G. Brickwedde, H. Van Dijk, M. Durieux, J. R. Clement, and J. K. Logan, J. Res. Natl. Bur. Stand. (U.S.) **64**, 1 (1960).

²⁰L. E. Wenger (private communication).

²¹R. E. Loehman, C. N. R. Rao, J. M. Honig, and C. E. Smith, J. Sci. Ind. Res. **28**, 1 (1969).

²²The analysis was performed by the Environmental and Materials Characterization Division of the Battelle Memorial Institute, Columbus, Ohio.

²³S. P. Denker, J. Phys. Chem. Solids **25**, 1397 (1964).

²⁴J. M. Honig, W. E. Wahnsiedler, and P. C. Eklund, J. Solid State Chem. **6**, 203 (1973).

²⁵L. Kaufmann, Trans. Metall. Soc. AIME (Am. Inst. Min. Metall. Pet. Eng.) **224**, 1006 (1962).

²⁶G. Gladstone, M. A. Jensen, and J. R. Schrieffer, in *Superconductivity*, edited by R. D. Parks (Dekker, New York, 1969), Chap. XIII.

²⁷W. L. McMillan, Phys. Rev. **167**, 331 (1968).

²⁸W. E. Wahnsiedler (private communication).

²⁹W. DeSorbo, Phys. Rev. **132**, 107 (1963).

³⁰J. Ferreira Da Silva, E. A. Burgemeister, and Z. Dokupil, Physica (Utr.) **41**, 409 (1969).

³¹R. Radebaugh and P. H. Keesom, Phys. Rev. **149**, 217 (1966).

³²R. R. Hake, Phys. Rev. **158**, 356 (1967).

³³V. L. Ginzburg, Zh. Eksp. Teor. Fiz. **30**, 593 (1956) [Sov. Phys.-JETP **3**, 621 (1956)].

³⁴K. Maki, Phys. Rev. **139**, A702 (1965).

³⁵A. Paskin, M. Strongin, P. P. Craig, and D. G. Schweitzer, Phys. Rev. **137**, A1816 (1965).

³⁶E. Helfand and N. R. Werthamer, Phys. Rev. **147**, 288 (1966).

³⁷B. Mühlischlegel, Z. Phys. **155**, 313 (1959).

³⁸J. L. Harden and V. Arp, Cryogenics **3**, 105 (1963).

³⁹A. L. Fitter and P. Hohenberg, in *Superconductivity*, edited by R. D. Parks (Dekker, New York, 1969), Chap. XIV.

⁴⁰D. Watanabe, J. R. Castles, A. Jostsons, and A. S. Mallin, Acta Crystallogr. **23**, 307 (1967).

⁴¹N. J. Doyle, J. K. Hulm, C. K. Jones, R. C. Miller, and A. Taylor, Phys. Lett. A **26**, 604 (1968).